

Mechanics of Chromosome Separation during Mitosis in *Fusarium* (Fungi imperfecti): New Evidence from Ultrastructural and Laser Microbeam Experiments

JAMES R. AIST and MICHAEL W. BERNS

Department of Plant Pathology, Cornell University, Ithaca, New York 14853, and Department of
Developmental and Cell Biology, University of California, Irvine, California 92717

ABSTRACT The anaphase-telophase spindle usually elongates, and it has been assumed that the spindle pushes the incipient daughter nuclei apart. To test this assumption, we used a laser microbeam to sever the central spindle of the fungus, *Fusarium solani*, and measured the rate of separation of incipient daughter nuclei. When the microbeam was aimed beside the spindle, separation occurred at a rate (8.6 $\mu\text{m}/\text{min}$) that did not differ significantly from the rate (7.6 $\mu\text{m}/\text{min}$) in unirradiated cells. But when the spindle was irradiated, it broke, and the separation was much faster (22.4 $\mu\text{m}/\text{min}$). Irradiation of cytoplasm lateral to one spindle pole resulted in a 1.5 $\mu\text{m}/\text{min}$ reduction in the rate (6.1 $\mu\text{m}/\text{min}$) of separation. From these and other data, we infer that extranuclear forces, presumably involving astral microtubules, pull on the incipient daughter nuclei and that the central spindle limits the separation rate. Astral microtubules are associated with the plasma membrane or, sometimes, with the rough endoplasmic reticulum. Most of the spindle microtubules that are present at metaphase are depolymerized during anaphase and early telophase.

Mitosis characteristically involves two phases of chromosome separation (1, 2). In phase I, daughter chromosomes move toward the spindle poles. In phase II, the spindle poles move farther apart as the central spindle elongates and the incipient daughter nuclei separate further. Phase II, though not universal, is of common occurrence among protozoa, algae, fungi, and higher plants and animals (1–5). The “Stämmkörper” theory of Belar (6, 7) has been almost universally accepted (1, 2, 5, 8) as an adequate explanation of the general mechanics involved in phase II: elongation of the central spindle is thought to push apart the daughter sets of chromosomes.

Although asters are commonly found at the spindle poles (higher plants are a notable exception) and may increase in size during phase II (9–11), they are routinely ignored in review papers on nuclear division (2, 8, 12–14). A few suggestions have been made that asters play an important role in chromosome separation (1, 4, 9–11, 15, 16), but experimental evidence for this concept as it applies to phase II (9) is scarce.

Mitosis in species of the fungus genus *Fusarium* exhibits a well-defined two-phase separation of chromosomes (17) within

an intact nuclear envelope (18). During anaphase, shortening of the kinetochore microtubules occurs as the kinetochores lead the chromosomes in their migration to the spindle poles (17, 18). Figs. 64–68 by Aist (17) indicate an increase of ~30% in spindle length during anaphase in a penultimate cell of *Fusarium oxysporum*. Astral microtubules become longer and more numerous at anaphase than at metaphase. Early telophase involves a considerable further elongation of the intact central spindle (up to three times its metaphase length) as astral microtubules form a conspicuous array in the cytoplasm. It was concluded that elongation of the central spindle near the end of mitosis provided the force necessary to separate the incipient daughter nuclei (18). The purpose of the present study was to test the validity of that conclusion. The rationale was that if the incipient daughter nuclei separate because the central spindle elongates between them, then by breaking the spindle immediately after the chromosomes have reached the poles at anaphase a decrease in the rate or extent of nuclear separation should be observed. An abstract of the experimental results has been published (19).

MATERIALS AND METHODS

Cultures of race T213 of *Fusarium solani* (Mart.) Sacc. (Ascomycete perfect stage: *Nectria haematococca* Berk. & Br.) were obtained from H. D. VanEtt (Cornell University). They were maintained on carboxymethylcellulose (CMC) agar and prepared for in vivo microscopic observation, irradiation, and subsequent fixation by the agar-slide method used by Aist and Williams (18).

The neodymium-YAG laser microbeam system used in this study was described by Strahs et al. (20). Cells were irradiated with a single pulse (100–150 ns) of green light (532-nm wavelength) sufficient to cause a phase-dark dot (~0.25 μm diameter) surrounded by a clear halo to appear in interphase nucleoli that were targeted during calibration procedures. Neutral density filters were used to adjust the impinging power of the laser to the desired level. This level of power was the minimal amount that would reliably sever the central spindle. Because the spindles in *F. solani* appear to be composed of two parallel adjacent strands (21), care had to be taken to include in Table I only irradiated nuclei whose spindle strands were lying one above the other during irradiation. This precaution ensured that both sides of these bipartite spindles would be broken when the spindle was irradiated, and that the spindle would not be affected when the nucleoplasm was irradiated. The cells were observed on a television monitor and videotaped before, during, and after each irradiation so that the accuracy and cellular effects of irradiation could be verified and migration rates determined.

Because optical clarity was greater in subapical cells than in apical cells, only second and third cells from the hyphal tip were included in the experiments. Twelve to fifteen mitoses in each of the four categories in Table I were recorded, and the first ten (chronologically) in which the necessary details could be clearly discerned in videotape replays were retained and analyzed. Spindle lengths at the moment of the laser pulse in all irradiated cells were determined first to establish a basis for measuring separation rates in unirradiated cells. Cells were irradiated within 5–10 s after all chromosomes had reached the poles, when the average spindle length was 7.7 μm . This spindle length then served as the starting point to measure the rate of separation of daughter nuclei in unirradiated cells. Separation rates were obtained by replaying the videotape sequences at $\times 10,400$ and measuring with a stopwatch the time required for the daughter nuclei to separate a further 6.7 μm after irradiation or, for unirradiated cells, after the spindle was 7.7 μm long. The standard distance, 6.7 μm , was then divided by the measured time to give $\mu\text{m}/\text{min}$. For statistical analyses, the measured times were used directly as raw data.




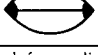
The speed with which events occurred during and after laser irradiation precluded effective 35mm photomicrography using a microflash attachment. Therefore, individual frames of the videotaped sequences were imaged at $\times 10,400$ on the TV monitor and photographed using a Nikon SLR 35mm camera mounted on a tripod. Although a considerable loss of image quality was unavoidably suffered by photographing individual frames, a precise record of high speed events could thus be correlated with elapsed time (i.e., Figs. 7, 10).

Samples for electron microscopy were obtained as follows. Small strips of tape were applied to the edges of 18 mm-square cover glasses. (The strips served as handles for the speedy removal of the cover glasses at a later stage.) The cover glasses were then placed over the mycelia and sealed with paraffin. After suitable cells had been selected and mapped for subsequent relocation (18), irradiations

were carried out as described above. Nuclei were observed and videotaped until ~5 s after irradiation to confirm that the targeting had been accurate. Then the slide was quickly removed from the microscope stage, the cover glass was removed, and the slide was immersed immediately in Fixative A (see protocol below) in a McJunkin staining dish (18). 10–20 s elapsed between irradiation and immersion in the fixative.

Freeze-substitution (22) could not be used to prepare irradiated specimens for electron micrography because the hyphae did not adhere to the cellulose-membrane supports after the cover slip had been removed following irradiation. Therefore, we were unable to take advantage of the superior ultrastructural preservation that the technique provides. The following chemical fixation protocol was developed and used for this study: (a) fix for 1 h at 22°C in Fixative A (contains 15 parts of CMC liquid medium, pH 6.75; 2.5 parts of 0.2 M sodium cacodylate, pH 7.0; 3 parts of 25% electron microscope-grade glutaraldehyde; and 20 parts of 0.02% aqueous uranyl acetate); (b) soak 10 min in half-strength (aqueous dilution) Fixative A; (c) embed in 1.5% water agar containing 0.01% uranyl acetate, at 48°C, and cool immediately to 22°C; (d) transfer squares of agar-embedded mycelium into stainless steel wire-mesh baskets sitting in 0.01% aqueous uranyl acetate; (e) soak three times for 20 min each in aqueous 0.01% uranyl acetate; (f) transfer into aqueous 0.1% OsO₄, plus 0.01% uranyl acetate for 30 min; (g) rinse two times, 15 min each, in aqueous 0.1% uranyl acetate; (h) soak in fresh aqueous 0.1% uranyl acetate for 1–3 h; (i) rinse twice in distilled

TABLE I
Effects of Laser Microbeam Irradiation on the Rate of Separation of Post-anaphase, Incipient Daughter Nuclei of the Fungus, *Fusarium solani*

Target	Schematic	Rate of separation* $\mu\text{m}/\text{min} \pm 1 \text{SD}$	Statistical comparisons‡
Unirradiated		7.6 \pm 1.2	A
Spindle		22.4 \pm 12.9	B
Nucleoplasm		8.6 \pm 1.7	A
Cytoplasm		6.1 \pm 1.5	C

* The rate was determined for a distance of 6.7 μm of separation for ten mitoses in each category.

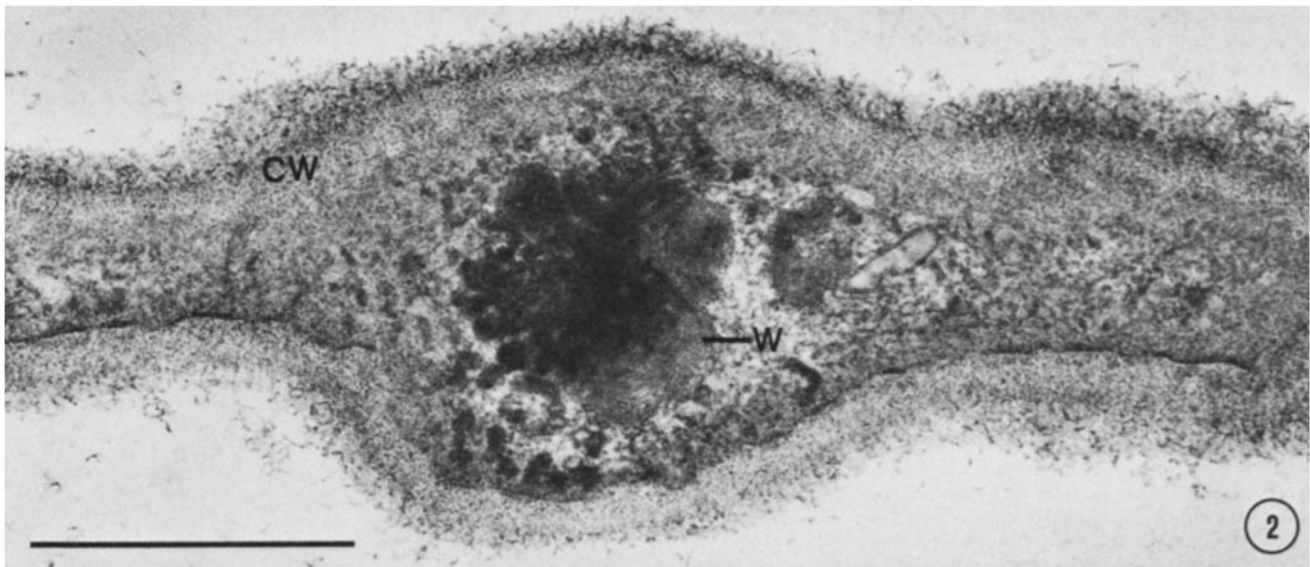
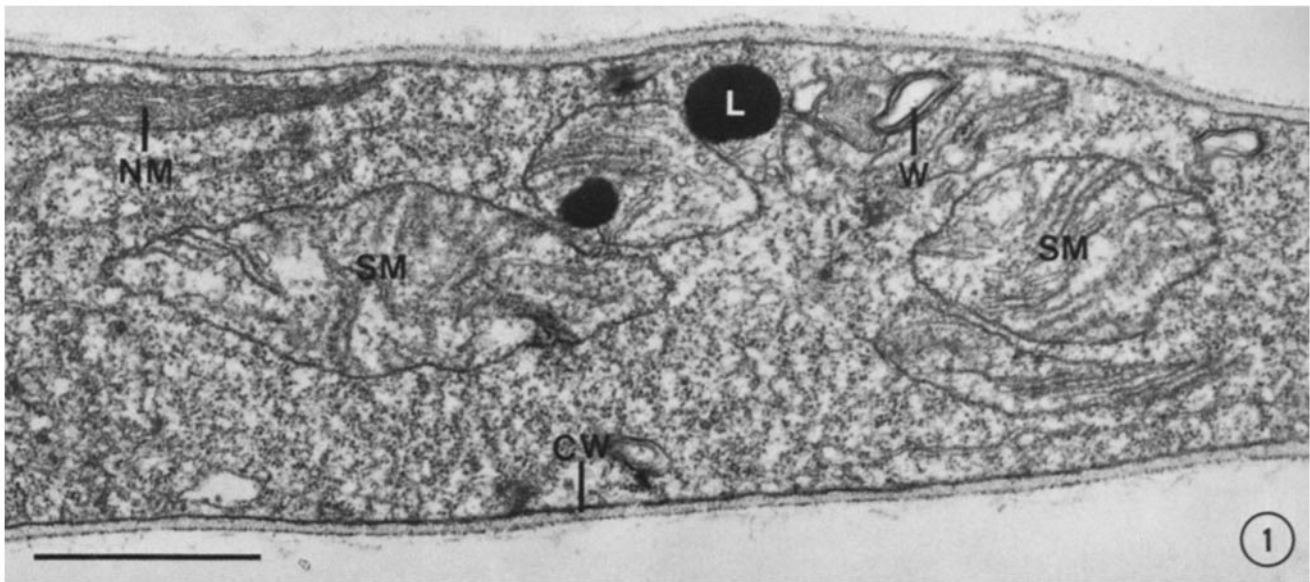
‡ Nonpaired Student's *t* test. Letters in common indicate no significant difference, whereas different letters indicate significance at $\leq 5\%$ level. These analyses were made using the actual times measured, not the rates.

TABLE II
Estimates of the Numbers of Spindle Microtubules at Various Stages of Mitosis in *Fusarium* spp.

Species	Stage	Specimen	Pretreatment	No. near pole 1	No. near center	No. near pole 2
<i>F. solani</i>	Metaphase	FS-4*	None	—‡	133	—
<i>F. solani</i>	Early anaphase	CF-5	Nucleoplasm irradiated	109	61	—
<i>F. solani</i>	Early telophase	CF-13	None	20	—	—
<i>F. solani</i>	Early telophase	CF-15	None	20	21	—
<i>F. solani</i>	Early telophase	CF-1	Spindle irradiated	23	—	26
<i>F. solani</i>	Early telophase	CF-2	Spindle irradiated	21	—	18
<i>F. solani</i>	Early telophase	CF-6	Nucleoplasm irradiated	11	20	16
<i>F. solani</i>	Early telophase	CF-7	Nucleoplasm irradiated	22	20	—
<i>F. solani</i>	Early telophase	CF-11	Cytoplasm irradiated	11	15	14
<i>F. solani</i>	Early telophase	CF-12	Cytoplasm irradiated	12	—	—
<i>F. oxysporum</i>	Metaphase	W-1	None	—	54	—
<i>F. oxysporum</i>	Metaphase	W-3	None	—	72	—
<i>F. oxysporum</i>	Telophase	W-4	None	22	—	—
<i>F. oxysporum</i>	Telophase	W-5	None	23	—	—
<i>F. oxysporum</i>	Telophase	W-6	None	11	12	—

* This specimen was freeze-substituted (22) in acetone containing 5% OsO₄ and 0.01% uranyl acetate.

‡ A dash indicates that sufficient appropriate sections were not available.



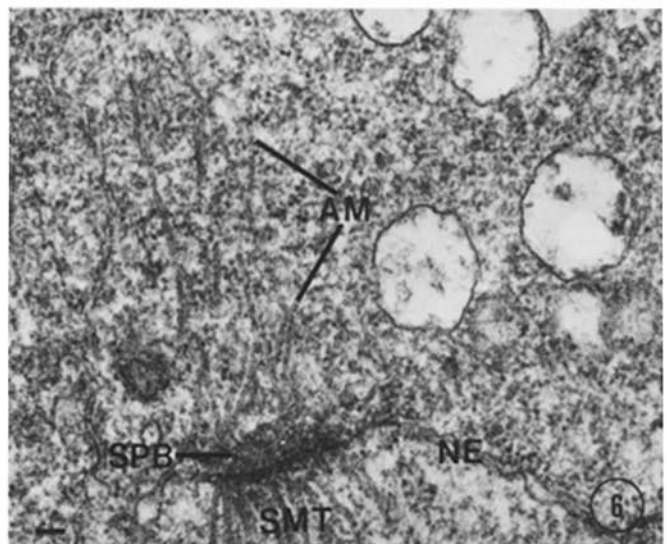
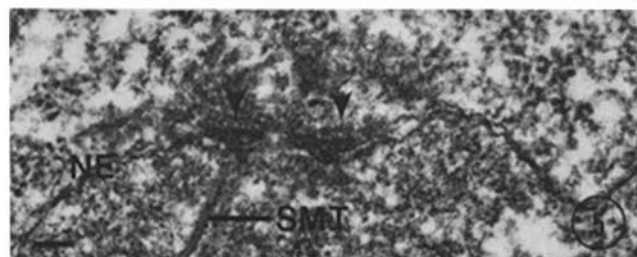
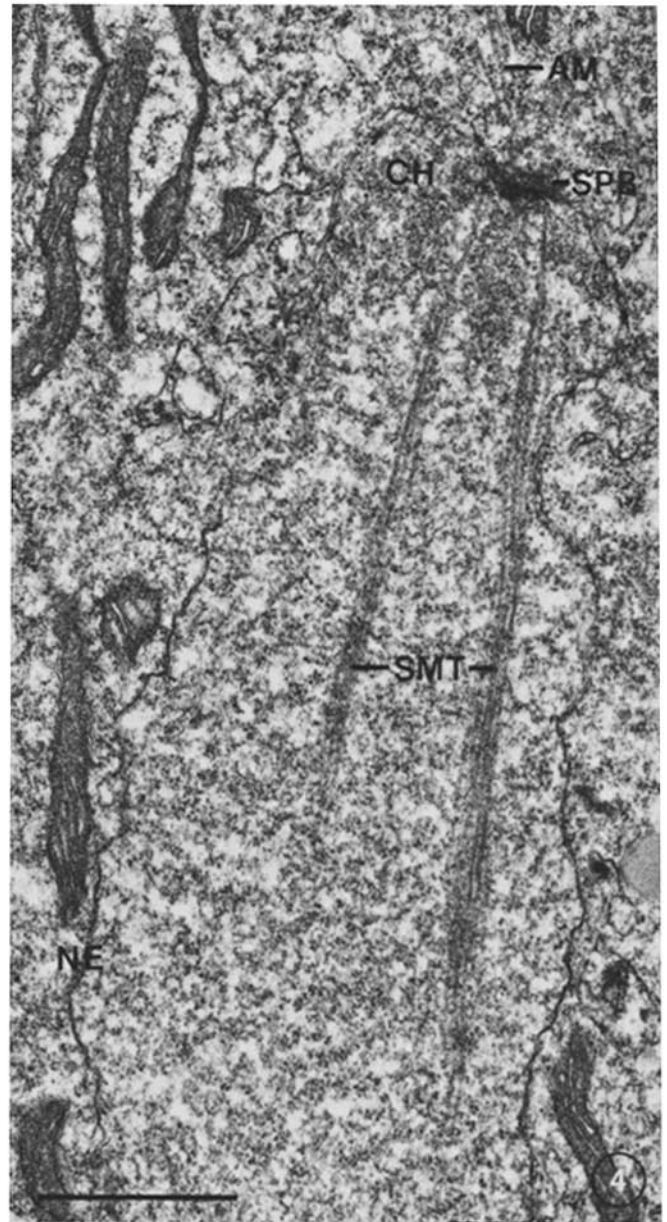
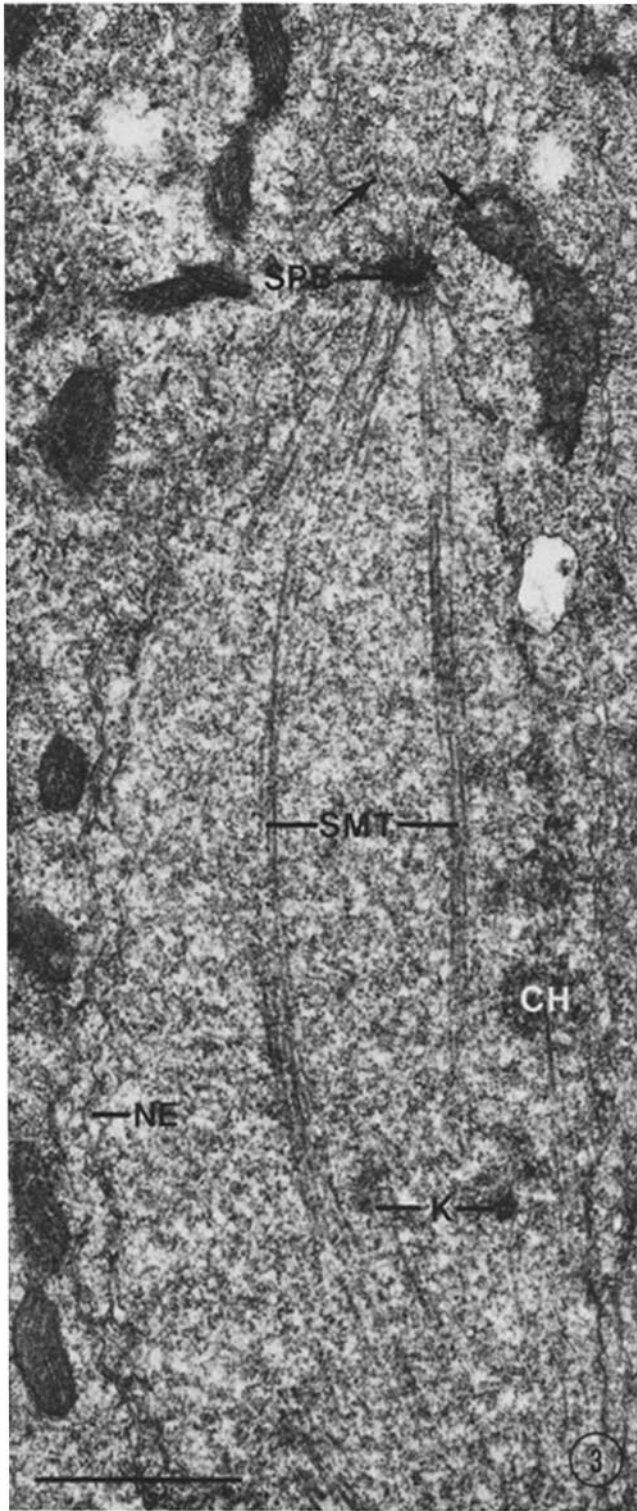
FIGURES 1 and 2 Electron micrographs showing nontarget damage above the focal point of the laser microbeam. Fig. 1 shows swollen mitochondria (SM), lipid bodies (L), and a membrane whorl (W) that resulted from irradiation. Cell wall, CW; normal mitochondrion, NM. Bar, 1 μm . $\times 30,000$. Fig. 2 shows a laser lesion subjacent to the plasma membrane where the laser beam entered the cell. This lesion is composed of densely staining globular material and membrane whorls. Bar, 1 μm . $\times 43,000$.

H₂O, 15–30 min each; (j) dehydrate in an acetone series; (k) embed in Epon-Araldite; and (l) polymerize at 60°C.

The plastic-embedded agar squares containing mycelium were transferred to 1 \times 3-inch glass slides for polymerization. After polymerization, the target cells were relocated, remounted, and thin-sectioned as described previously (18). After uranyl acetate and lead citrate poststaining, electron micrographs were taken of complete or nearly complete series of adjacent sections through both spindle pole bodies (SPBs; 18) and the central spindle of eight mitotic apparatuses, two from each of the four experimental categories (Table I). Also, one early anaphase nucleus that had been irradiated just inside the nuclear envelope about equidistant from the SPBs was included.

Two methods were used to estimate numbers of spindle microtubules on prints at $\times 12,500$ –50,000. Microtubules in cross- and near-cross sections were counted directly on prints from two adjacent sections after marking each microtubule profile with an ink dot. The average of the two counts, which varied by only 1–3 microtubules, was taken as the best estimate. For near-cross sections, viewing the prints at a low angle with the microtubules viewed nearly end-on was of great help in identifying valid profiles. To help avoid inclusion of kinetochore microtubules in counts of telophase spindle microtubules, counts were made only on micrographs in which the center of the bundle was at a distance from the SPB representing 0.5–3.0 μm . For estimates from near-longitudinal sections, only complete series of serial sections through spindles were used. Near spindle poles,

FIGURES 3–6 Electron micrographs depicting various aspects of the mitotic apparatus in *F. solani*. The mitotic apparatus in the nucleoplasm-irradiated, early anaphase nucleus in Fig. 3 is composed of two main strands of spindle microtubules (SMT), spindle pole bodies (SPB), astral microtubules (arrows), and chromosomes (CH) with kinetochores (K). Nuclear envelope, NE. Bar, 1 μm . $\times 26,900$. Fig. 4 is early telophase in an unirradiated cell and shows two main strands of SMT, CH near the SPB, and astral microtubules (AM). Bar, 1 μm . $\times 26,900$. In Fig. 5, the SPB appears double (arrowheads) at early telophase. Bar, 0.1 μm . $\times 52,000$. Fig. 6 (same nucleus as in Fig. 3) suggests the considerable extent of the early anaphase aster as evidenced by the numerous AMs that are projecting forward from the SPB. Bar, 0.1 μm . $\times 41,500$.



a pair of lines perpendicular to the spindle and separated by a standard distance (0.15–0.5 cm, depending on the magnification) were first drawn on each print at a distance from the SPB representing 0.375 μm and 0.5 μm . Then, the number of microtubule profiles that crossed each line in each print was counted, using a $\times 3$ magnifier, and totalled. The average of these two totals was used as the best estimate. For estimates near the spindle center in near-longitudinal sections, the two lines were drawn at set distances from the SPBs, near the midpoint of the spindle. These lines were 0.5 cm apart on the prints, regardless of magnification. Counts were made and averaged as for polar estimates. Both the direct count method and the line count method gave comparable and repeatable estimates. However, any counts from near-cross or near-longitudinal sections have the potential to underestimate somewhat the number actually present because of vertical stacking of some microtubules within the section. Therefore, the data in Table II are intended only as rough estimates of microtubule numbers. Electron micrographs of several nuclei of *F. oxysporum* from a previous study (18) were included in these estimates for comparison.

RESULTS

Several side effects of laser irradiation were noticed. Routinely, there was a very slight and immediate contraction of some cytoplasm toward the targeted area. Frequently a mitochondrion 5–10 μm away from the path of the laser beam would be immediately jerked toward or away from the target area at the moment of the laser pulse. Mitochondria within the path of the laser beam swelled rapidly (Fig. 1). This sensitivity to green laser light probably reflects the cytochrome content of mitochondria, since cytochromes absorb heavily in the green wavelengths (23). The laser pulse always induced the cells to form wall appositions (24) within a few minutes. This reaction was apparently a response to considerable localized damage (Fig. 2) in the first 1 μm of cytoplasm below the cell wall where the converging laser beam entered the cell. Below this layer of damaged cytoplasm was a 1–2 μm thick layer of undamaged cytoplasm, followed by a roughly spherical region of laser damage $\sim 0.4 \mu\text{m}$ in diameter (Figs. 11–15).

Despite the side effects, irradiated cells consistently remained alive and damage remained localized. All nuclei continued to divide, and they proceeded not only into interphase, but those that were monitored further completed the next mitotic cycle as well. Moreover, the growth of hyphal tip cells seemed unaffected when these cells were irradiated subapically. In summary, the observed side effects of laser irradiation were highly localized to the irradiated site and did not interfere detectably with overall cellular processes.

The general features of mitosis in *F. solani* were described from observations of living cells by Thielke (25) and closely resemble those in *F. oxysporum* (17, 18). Mitosis (Figs. 3–8) is intranuclear, and the mitotic apparatus includes a microtubular spindle, disc-shaped or hemispherical SPBs, discrete chromosomes, and astral microtubules. Videotape replays clearly showed that during prophase the daughter SPBs migrate apart in a direction perpendicular to the long axis of the cell, until they reach a position near the opposite sides of the cell. When the half-spindles have become aligned to form a complete spindle, the spindle elongates as the entire mitotic apparatus rotates slowly to an orientation nearly parallel to the cell's long axis. This metaphase stage lasts for ~ 2 –3 min and is character-

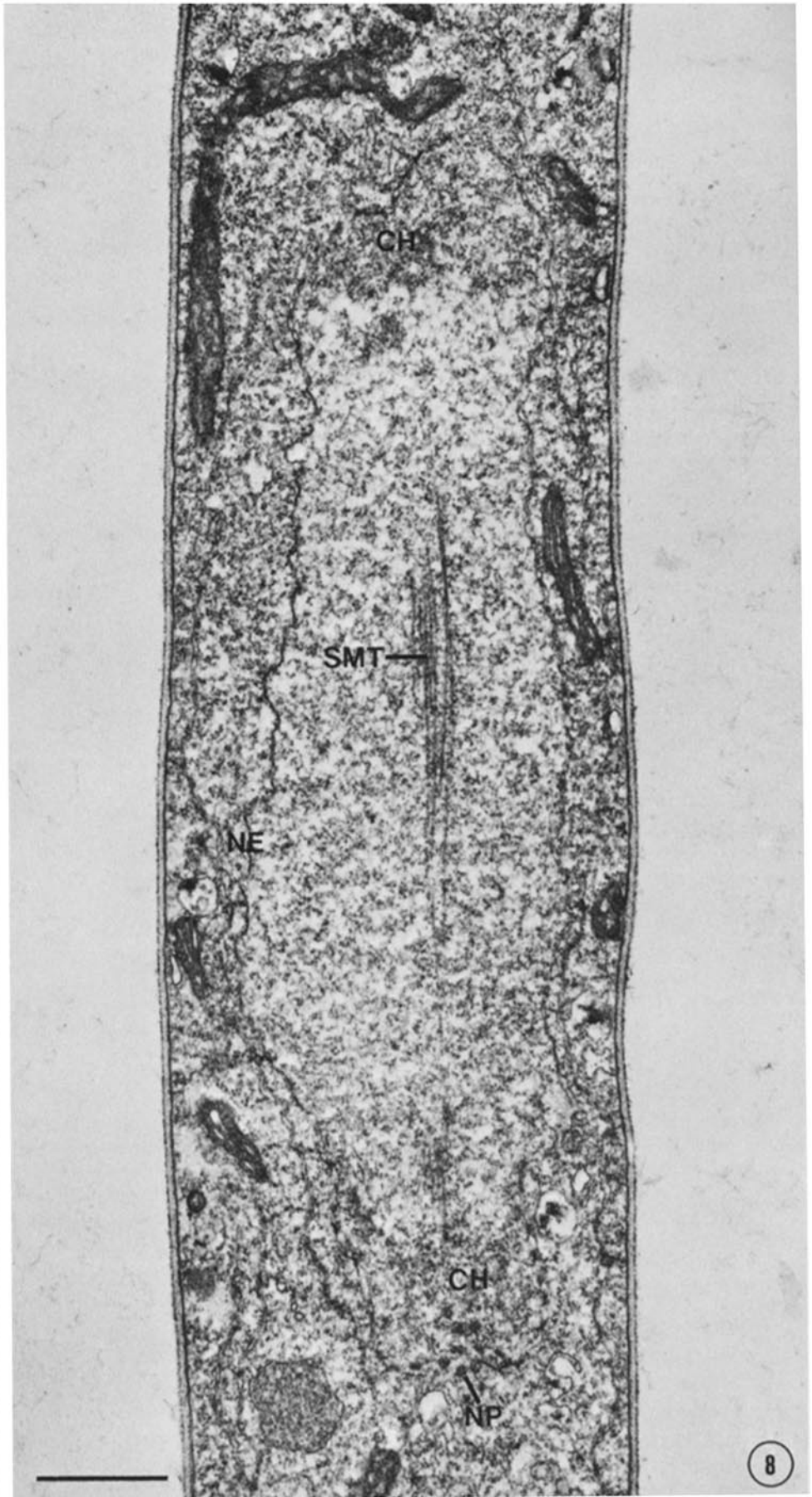
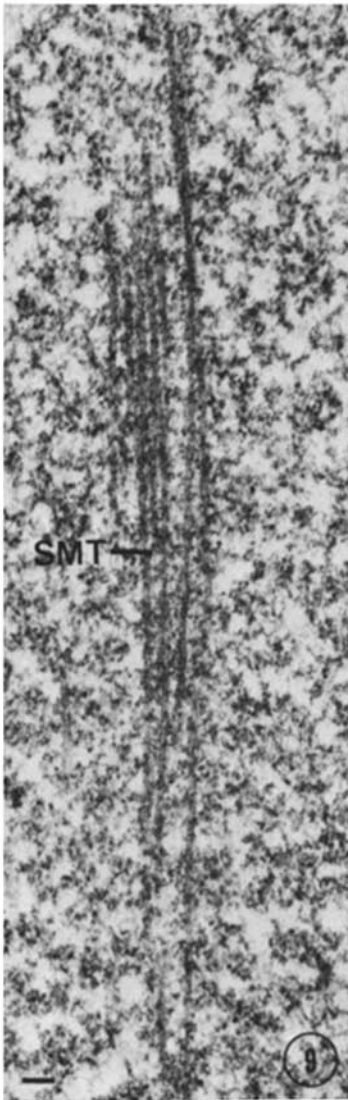
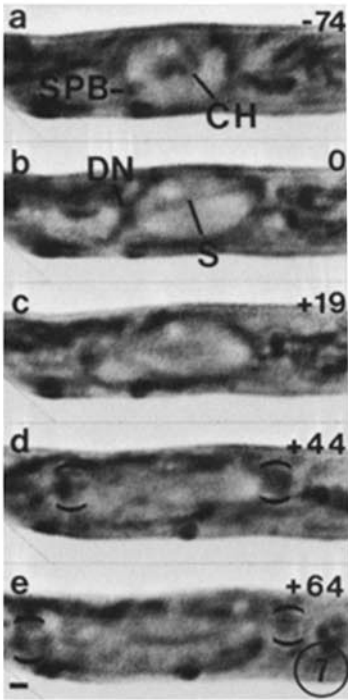
ized by intermittent rotational movements of the mitotic apparatus.

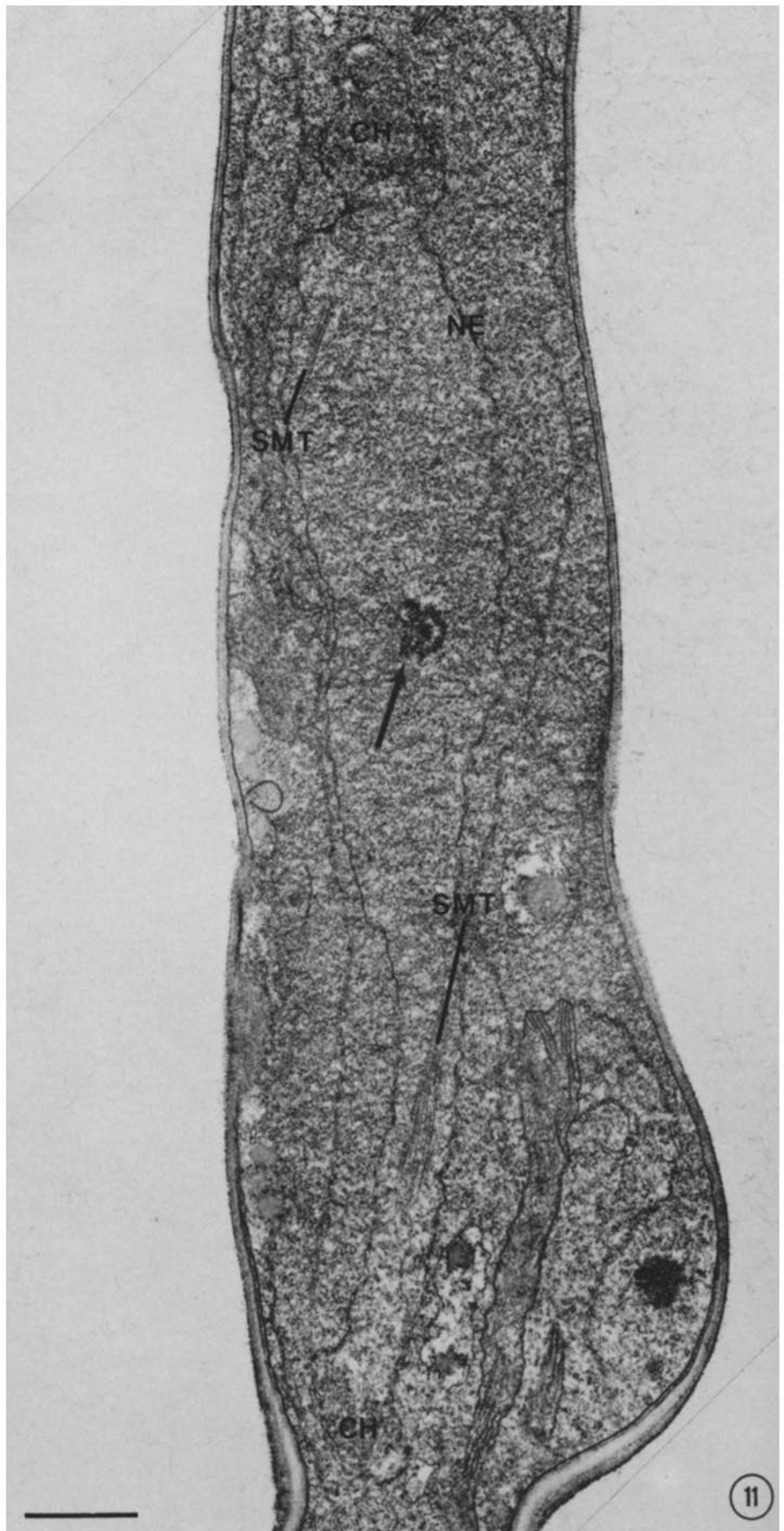
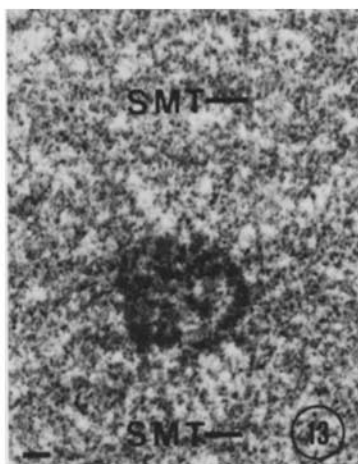
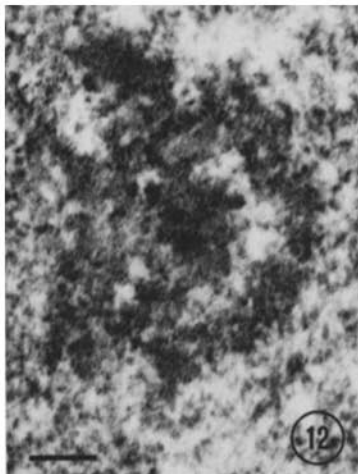
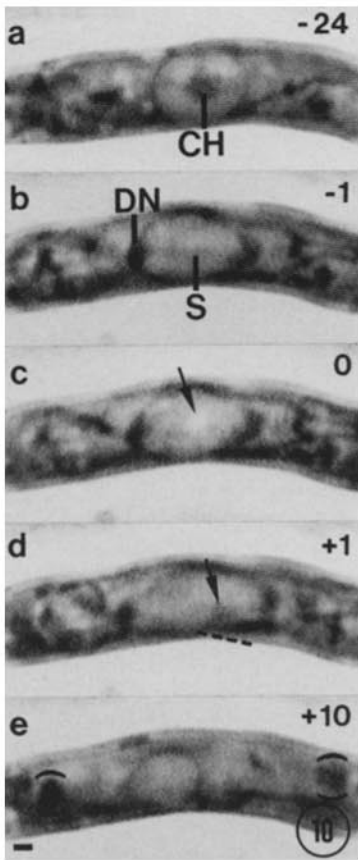
During anaphase, an ~ 20 –25% increase in the length of the spindle occurs as the daughter chromosomes migrate to their respective poles. By early anaphase (Figs. 3 and 6) prominent asters have developed. In the example shown in Figs. 3 and 6, only two or three (perhaps 10% of the total) of the astral microtubules were found to be oriented back toward the opposite pole. The SPBs of this nucleus were perpendicular to the cell's long axis, and none of the astral microtubules were found, in serial sections, to even approach the vicinity of the plasma membrane. In twelve adjacent serial sections (e.g. Fig. 3), ten kinetochores were found connected to one spindle pole, seven to the other. There was one kinetochore per chromosome and one microtubule per kinetochore.

One interesting feature of the mitotic apparatus of *F. solani* is that often the spindle is basically bipartite from early anaphase (Fig. 3) through early telophase (Fig. 4). The spindles shown in Figs. 3 and 4 each had an additional strand of two to four microtubules in another plane of section. SPBs frequently appeared double at early telophase (Fig. 5), but a specific spatial relationship between the two most prominent bundles of spindle microtubules and the two SPBs at any one pole was not apparent. Videotape analyses of anaphase demonstrated that chromatids could migrate along both sides of the bipartite spindles toward the poles. Between anaphase and the middle of phase II, the main strands of the spindle coalesced into a single, narrow bundle of microtubules (Fig. 8).

Incipient daughter nuclei in unirradiated cells (Fig. 7) separated at an average rate of 7.6 $\mu\text{m}/\text{min}$ (Table I). During this separation, a bundle of central spindle microtubules (Figs. 8 and 9) elongated between the SPBs. When the spindle was irradiated (Fig. 10c), the microbeam broke the spindle and the incipient daughter nuclei separated at an accelerated average rate of 22.4 $\mu\text{m}/\text{min}$. (Table I). Moreover, these nuclei usually migrated farther apart than did those in unirradiated cells. Successful breakage of the spindle was verified in videotape replays and was characterized by the appearance of a phase-clear region in the spindle where it was irradiated and, frequently, by the subsequent appearance of a dark globule (Figs. 10d and 11) that replaced the clear region. One or both of the two shafts of the broken spindle routinely rotated (Figs. 10d and 11) such that they were no longer oriented toward the opposite pole. In five or six additional nuclei (not included in Table I), only one of the strands of the spindle was irradiated, resulting in rotation of the broken halves of the irradiated strand, while the other strand continued to elongate with the nucleus. Once they rotated, the broken spindle shafts (of either bipartite or coalesced spindles) maintained their new, oblique orientation through most or all of the subsequent separation phase (Fig. 11). Some incipient daughter nuclei jerked abruptly apart an additional 2–3 μm immediately upon spindle irradiation, while others either exhibited only a gradual acceleration or paused for 2–3 s before accelerating rapidly. The lesion created by the focused laser beam had a coarsely granular

FIGURES 7–9 Aspects of mitosis in unirradiated cells. Fig. 7: time-lapse series of a living cell of *F. solani*: a is at metaphase; b–e are progressively later telophase stages of the separation of incipient daughter nuclei (in parentheses). These are phase-contrast, videotape images. Relative times (in seconds) are in the upper right of each frame. Incipient daughter nuclei, DN; and spindle, S. Bar, 1 μm . $\times 2,250$. Fig. 8: a nucleus fixed ~ 20 sec after anaphase. Note the (typical) retention of the intact nuclear envelope and the narrow bundle of SMT. Nuclear pore, NP. Bar, 1 μm . $\times 20,900$. Fig. 9 is an enlargement of the SMT in Fig. 8. Bar, 0.1 μm . $\times 41,800$.





ultrastructure and was heavily stained (Figs. 11–13). In only one of the two spindle-irradiated nuclei that were examined by electron microscopy did a few microtubules remain in the center of the nucleus, near the lesion (Fig. 13); the others were carried along with the rapidly separating SPBs.

When the microbeam was aimed at the nucleoplasm, beside the spindle (Fig. 14), the incipient daughter nuclei separated at an average rate of 8.6 $\mu\text{m}/\text{min}$, which was comparable ($P = 0.1$) to the rate in unirradiated cells (Table I). No ultrastructural alterations were observed in these spindles (Fig. 15), although the characteristic laser lesion was produced. Videotape replays verified that the central spindle remained intact during further separation of the nuclei.

Irradiations of the cytoplasm lateral to one of the spindle poles were included as a check for general, nonspecific effects of the laser pulse on phase II. Our intent was to irradiate as close as possible to the nucleus without damaging the astral microtubules. Nevertheless, these irradiations resulted in a small but statistically significant ($P = 0.025$) reduction (from 7.6 $\mu\text{m}/\text{min}$ to 6.1 $\mu\text{m}/\text{min}$) in the rate of separation of incipient daughter nuclei (Table I). As with nucleoplasm irradiations, a laser lesion was produced (Fig. 16) and the spindle remained intact during further separation. No ultrastructural damage to the conspicuous array of astral microtubules that typifies anaphase and telophase (Figs. 17 and 18) was detected. The limited extent of adjacent serial sections and the broad divergence of astral microtubules prevented quantitation of the microtubules of the asters. However, the numbers and lengths of astral microtubules in cytoplasm-irradiated and unirradiated cells appeared to be similar. There were, of course, laser-damaged (swollen) mitochondria (Fig. 16) near the cytoplasmic target area.

The distal ends of some of the astral microtubules closely approached the plasma membrane (Figs. 17, 19, and 20). These microtubule terminations were embedded in a flocculent matrix (Fig. 17), or flared out at the end (Fig. 19), or both (Fig. 20). Fourteen early telophase asters were analyzed (in serial sections that included the entire SPBs as well as regions including and beyond all microtubule terminations indicated) for terminations of astral microtubules. Four had one termination, four had two terminations, three had three terminations, two had four terminations and one had seven terminations of astral microtubules, all near the plasma membrane. One astral microtubule ended in a flared terminus adjacent to a sheet of rough endoplasmic reticulum (Fig. 21). All of the early telophase spindles were slightly angled with respect to the longitudinal cells axis (Figs. 14 and 16). Also, the SPBs were always at an angle with respect to the spindles (Figs. 16 and 18), such that the two SPBs of any one nucleus were oriented toward opposite sides of the cell (Fig. 16). The one exception is the mitotic apparatus in Fig. 18, in which both SPBs were facing the same side of the cell. Without exception, the SPBs

were found to have astral microtubules associated with the plasma membrane on only the side of the cell which they faced. Some of these associations were anterior to the SPB, and others were posterior. One of two “free” terminations of astral microtubules that were found was flared: the other was undifferentiated.

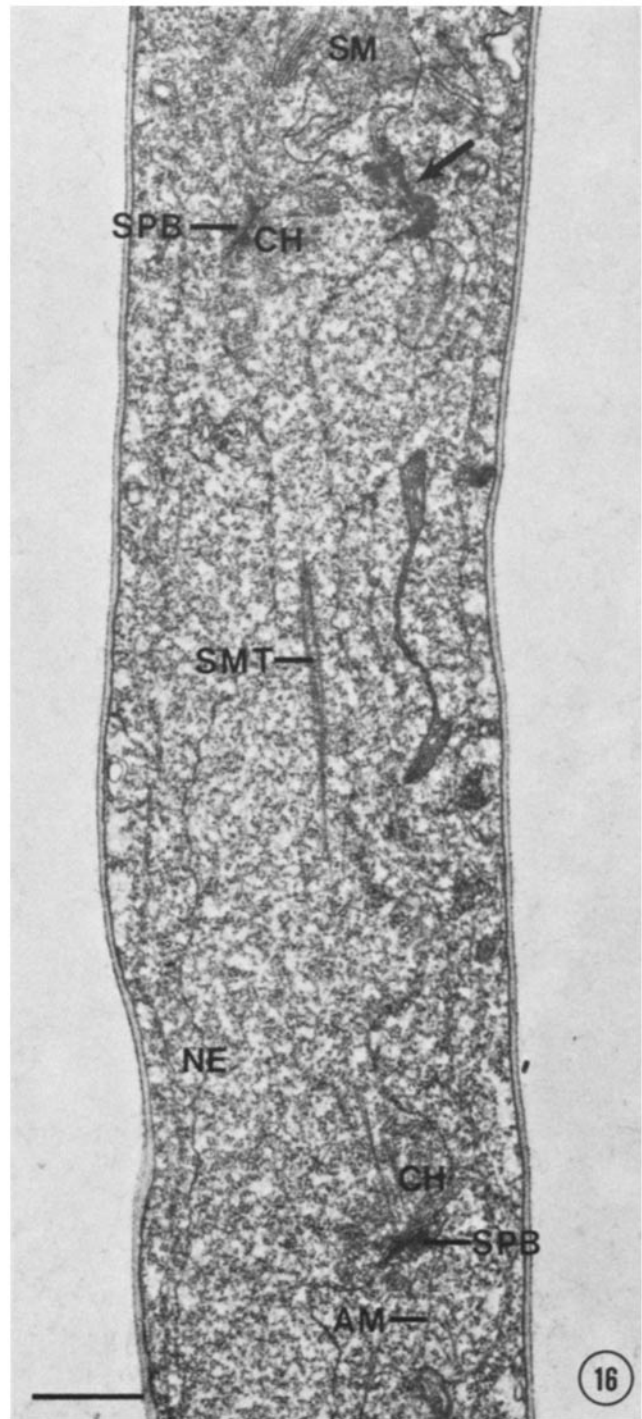
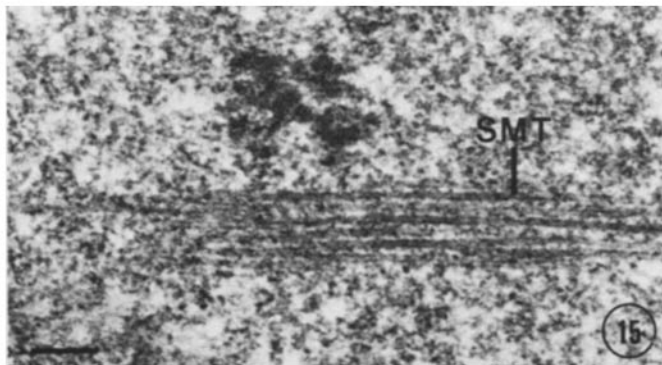
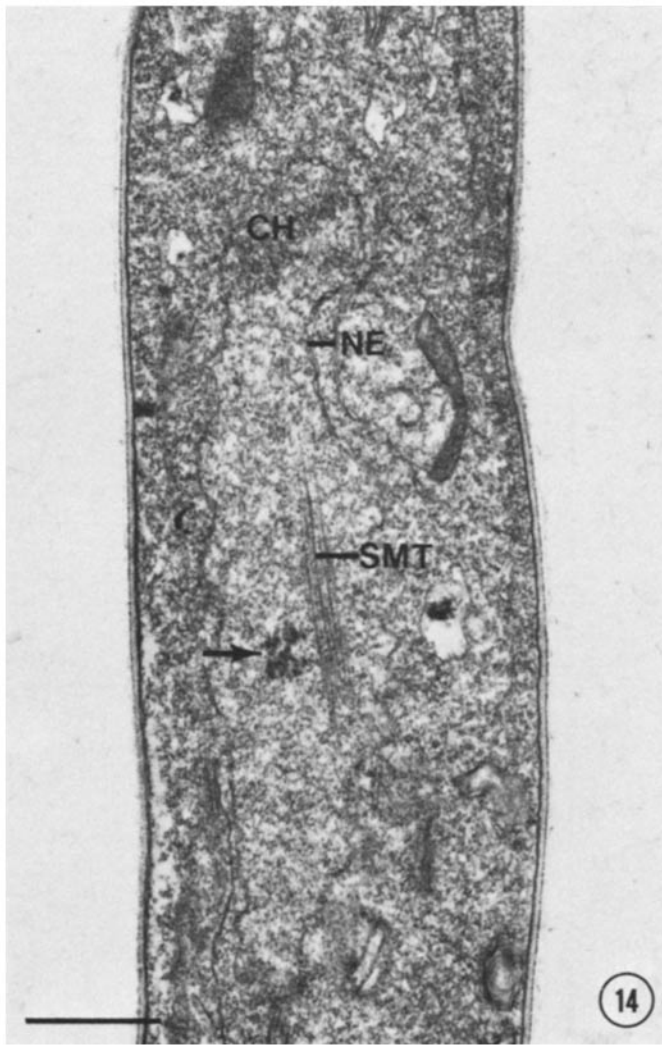
Astral microtubules were commonly at least 2–3 μm long, and many were $>5 \mu\text{m}$ long. As estimated 60–80% of the total number of astral microtubules at a pole were oriented anteriorly, 15–35% posteriorly, and 5% laterally with respect to the SPB. The mitotic apparatus in a branching, penultimate cell characteristically migrates toward and into (at least partially) the base of the branch during phase II, where the leading nucleus takes up permanent residence as the trailing nucleus migrates back into the main hypha. Fig. 18 is taken from a section through such a mitotic apparatus and shows that the astral microtubules splay out into the base of the branch. Such microtubules may come to within $\sim 12 \text{ nm}$ of the plasma membrane (Fig. 22).

Rough estimates of the numbers of spindle microtubules in *Fusarium* spp. are presented in Table II. It is obvious that about two-thirds of the spindle microtubules are depolymerized between metaphase and telophase. Depolymerization of the shortening kinetochore microtubules could account for only a very small percentage of this dramatic decrease; only about four to twelve kinetochore microtubules are attached to each pole (18; and present results). The unusually high estimate of 133 for the freeze-substituted metaphase nucleus may have been due to the superior preservation of microtubules afforded by this technique (22), or to a higher number having been present in vivo at metaphase in *F. solani*, or to both. Among telophase nuclei in both species there seem to be two distinct categories of spindles; some have a higher number of spindle microtubules (20–23 estimated) and some a lower number (11–16 estimated). This difference was especially consistent near the spindle poles. With the possible exception of one nucleus (CF-6 in Table II), the number of microtubules at the centers of telophase spindles was comparable to the number at the poles.

DISCUSSION

The dramatic increase in the rate of separation of incipient daughter nuclei when the spindle was broken was quite unexpected and required a rethinking of current concepts about the mechanics of chromosome separation, especially in *Fusarium* spp. The most obvious interpretation is that extranuclear forces are pulling on the SPBs during phase II. This interpretation is further supported, albeit indirectly, by the observation that laser damage to the cytoplasm beside one of the SPBs slowed the rate of separation, and could be directly tested by additional experiments in which the asters are irradiated. Previous inferences and speculations about such forces (4, 10, 15, 16, 26) are

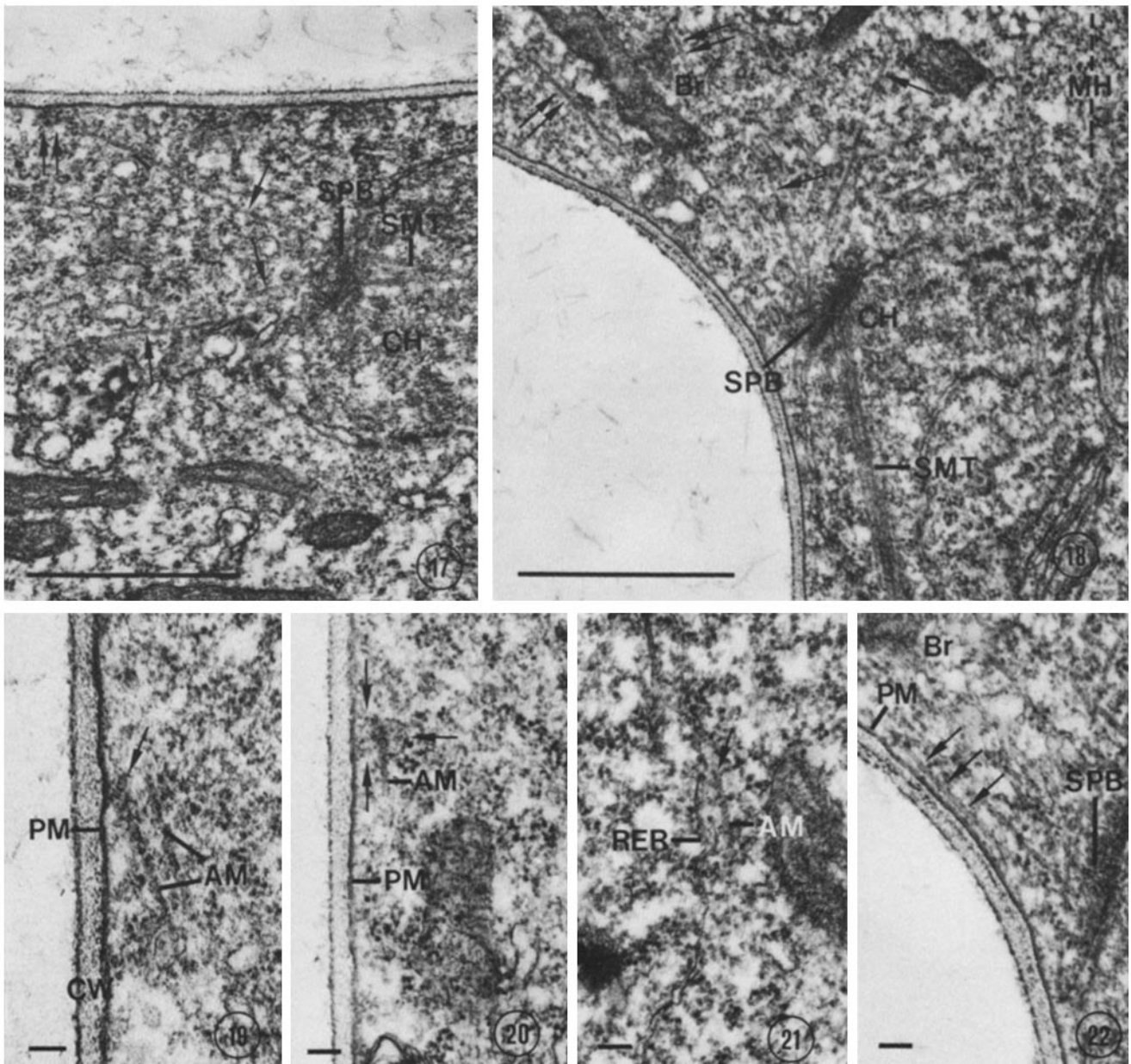
FIGURES 10–13 These cells were irradiated near the center of the early telophase spindle. Fig. 10: a time-lapse series of a living cell in which the spindle was severed: a is at metaphase; b shows the intact, early telophase spindle (S); c shows the residual fluorescence (arrow) incited by laser irradiation; d shows one-half of the broken spindle (parallel to the dashed line) and laser-damaged material (arrow); and e shows the incipient daughter nuclei (in parentheses) upon completion of separation. These are phase-contrast, videotape images. Relative times (seconds) are in the upper right of each frame. Bar, 1 μm . $\times 2,250$. Fig. 11: an early telophase cell fixed 10–20 s after the spindle was severed by the laser. The strands of broken SMT have rotated, and an area of laser-damaged material (arrow) lies between the incipient DN. Bar, 1 μm . $\times 17,900$. Figs. 12 and 13 show, respectively, the ultrastructural details of, and two residual SMT associated with, the laser lesion in Fig. 11. Fig. 12: bar, 0.1 μm ; $\times 88,400$. Fig. 13: bar, 0.1 μm ; $\times 37,800$.



FIGURES 14-16 Electron micrographs of cells irradiated in the nucleoplasm or cytoplasm. Fig. 14 is an early telophase cell fixed 10-20 s after the nucleoplasm was irradiated. The laser-damaged material (arrow) lies next to the SMT, which appear unaltered. Bar, 1 μ m. \times 17,900. Fig. 15 is an enlargement of the spindle in Fig. 14. The SMT are not detectably altered, even though the laser lesion is close by. Bar, 0.1 μ m. \times 49,800. Fig. 16 is a cell fixed 10-20 s after the cytoplasm was irradiated adjacent to the incipient daughter nucleus at the top. Note the area of laser-damaged cytoplasm (arrow) and the SM (swollen mitochondrion) nearby. The SPB are slanted toward opposite sides of the cell. Bar, 1 μ m. \times 14,900.

supported by our results. Our interpretation would explain why the entire mitotic apparatus, at least in several fungi, can migrate or oscillate in the cell (10, 17, 18, 27). It also would suggest why, during normal mitosis, the elongated, telophase spindle sometimes snaps in the middle with a recoil of the free ends toward the respective spindle poles (17, 25): the spindle is apparently under tension from polar forces pulling in opposite directions. Such polar forces could also contribute to coales-

cence of the strands of spindle microtubules into a single, tightly packed bundle at telophase by putting tension on them. The postulated polar forces would be intermittent, resulting in oscillations of the mitotic apparatus (10, 18). In the present experiments the intermittent nature of the polar forces would explain the observed difference in elapsed time between breakage of the spindle and acceleration of incipient daughter nuclei; some jerked apart immediately, whereas others hesitated before



FIGURES 17-22 Ultrastructural aspects of asters in early telophase nuclei. Fig. 17 shows a typical aster in an unirradiated cell. AM (arrows) radiate from the SPB into the cytoplasm, where one (double arrow) terminates in a small cloud of flocculent material near the plasma membrane. Bar, 1 μm . $\times 33,200$. In Fig. 18, the mitotic apparatus was about to enter a hyphal branch (Br). The cell had been irradiated in the cytoplasm beside this SPB (the laser lesion is out of the plane of section, to the center right). This typical aster has the normal array of microtubules (arrows), some of which (double arrows) have splayed out into the branch, ahead of the SPB which is slanted toward the branch. The main hypha (MH) is oriented parallel to the dashed lines. Bar, 1 μm . $\times 32,000$. Figs. 19-22 show various spatial associations of AM with other cell structures. In Figs. 19 and 20, two adjacent, posteriorly oriented microtubules terminate at or near the plasma membrane (PM), with either a flared terminus (arrow, Fig. 19) or a swollen terminus embedded in flocculent material (arrows, Fig. 20). The flared microtubule terminus (arrow) of the anteriorly oriented microtubule in Fig. 21 ends at a sheet of rough endoplasmic reticulum (RER). Fig. 22 shows AM of the aster in Fig. 18 in a different section. One of these microtubules (arrows) lies within 12 nm of the PM and extends into the branch (Br). All of these microtubules were traced back to the SPBs in adjacent serial sections, which also verified their terminations as illustrated. Bars, 0.1 μm . Fig. 19, $\times 59,700$; Figs. 20 and 21, $\times 51,900$; Fig. 22, $\times 50,000$.

accelerating rapidly. The existence of polar forces would help ensure that incipient daughter nuclei could separate even if a prominent central spindle did not form, as occurs in aberrant mitoses in older cells of *F. oxysporum* (Aist, unpublished observations) and in cultured newt cells (28).

The astral microtubules are inferred to play a role in the deployment of these putative polar forces because they are

attached to the SPB and increase in number and length at an appropriate time (10, 16, 18). In addition, they seem to play a role in migration of interphase nuclei, which apparently involves a force transmitted to the SPB (18, 26, 29-31). Since fungi contain actin (32), as well as microfilaments that are sometimes closely associated with microtubules (33), it is possible that the polar force is generated by a microfilament-based

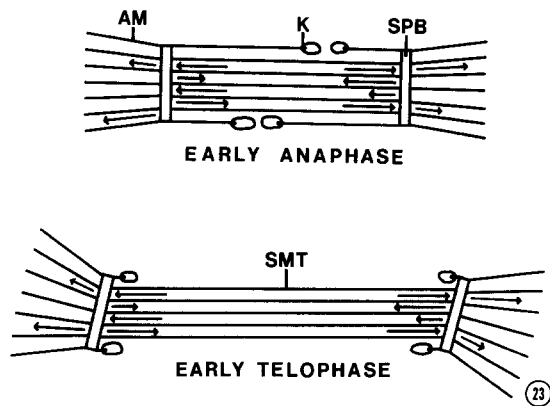


FIGURE 23 Diagrammatic representation (not to scale) of forces postulated to act on the SPB during chromosome separation in *F. solani*. The numbers and lengths of the arrows represent rough approximations of the magnitudes and directions of the forces. The distinguishing features of this model are the astral forces and opposing (resistive) spindle counterforces that were revealed primarily by breaking the spindle at early telophase.

motility system. The residual ability, albeit reduced, of fungal nuclei to divide (34, 35) in the presence of antimicrotubule agents may be evidence of such a force-generating system, and suggests that the role of microtubules could be largely one of facilitating net force production by maintaining the orientation of microfilaments more or less parallel to the hyphae, as suggested by Heath (29). However, this concept alone could not explain how the two poles could be pulled in opposite directions at the same time. It seems more likely that the main force would be transmitted from microfilaments to the astral microtubules by an interaction between these two cytoskeletal elements (36, 37). Since asters can move small particles toward their centers (1), it is not difficult to imagine that an interaction between a stationary, cytoskeletal element (e.g. microfilaments) and astral microtubules would propel the aster forward. The inherent polarity of microtubules (1) could somehow confer opposite directionality to the forces operating on the two SPBs, since most of the microtubules of the two opposing asters are oriented forward, away from the nucleus. Unfortunately, the ultrastructural preservation of microfilaments in our study was inadequate to shed light on this possibility; microfilaments were routinely detected only at developing septa and in Spitzkörpern, where they are known from freeze-substitution studies to occur in abundance in *F. solani* (Aist and Berns, unpublished observations) and in *Fusarium acuminatum* (38).

The close associations observed here between astral microtubules and the plasma membrane suggest that some of these microtubules are anchored near the cell surface. Cytoplasmic microtubules have been shown to be attached or associated with the plasma membrane of various plant cells by means of flared or swollen termini (38–40). An alternative possibility is that these plasma membrane-associated microtubules receive a motile force by interacting with an actin-myosin complex like the one associated with the plasma membrane of ascites tumor cells (41). In support of this idea is Howard's (38) illustration of microfilaments associated with the plasma membrane of *F. acuminatum*.

Cytoplasmic irradiation may have reduced the rate of separation of incipient daughter nuclei by damaging a microfilament system or the mitochondria in the vicinity of the aster and thereby inhibiting one or more of the components neces-

sary to generate the motile force; a direct ultrastructural effect on astral microtubules was not apparent. Griffin et al. (42) found that cytoplasmic irradiation of *Physarum polycephalum* with a laser interrupted cyclosis which, in this organism, is based on a microfilament system (43).

The other major interpretation of these data is that the central spindle in *F. solani* acts as a mechanical governor that limits the rate at which the SPBs (and, therefore, the incipient daughter nuclei) separate during phase II. This role of the spindle was inferred by Girbardt (10) on the basis of oscillations and migrations of mitotic nuclei of the Basidiomycete, *Trametes versicolor*, and by Crackower (34) on the basis of nuclear behavior in the Ascomycete, *Aspergillus nidulans*, in the presence of a spindle poison, griseofulvin. Our study provides direct confirmation of this regulatory role of the central spindle. Forer (12) has postulated a related role for kinetochore microtubules during poleward migration of chromosomes in anaphase, but the relevance of our results to his postulate is unclear.

Forces generated by elongating spindles are usually thought to result from growth of the microtubules, their lateral interactions (sliding) or both (1, 8, 44). In view of these results, we must consider the possibility that one or both of these mechanisms limits the rate of separation of the incipient daughter nuclei. The microtubule counts lend support to the view that microtubule growth occurs, since most telophase nuclei had similar numbers of microtubules near both the poles and the center of the spindle. According to this concept, the rate of polymerization of (presumably) continuous microtubules could limit the rate at which the nuclei separate. The continuous microtubules would have to be somehow protected from the depolymerizing conditions that give rise to the decline in numbers of microtubules that precedes telophase. The data do not exclude the possibility that microtubule sliding may occur also. Extensive microtubule tracking data would help clarify these important aspects of spindle ultrastructure.

The concept that the spindle generates counterforces that resist the pull on the SPBs should not be taken to imply that the spindle is not capable of generating a pushing force as well. Certainly in situations where the elongating central spindle becomes bent or fractured (6, 7, 17, 45, 46), there is reason to think that it is pushing. The central spindle in the Ascomycete, *Ceratocystis fagacearum*, is sometimes curved temporarily during its elongation phase (17). This curvature could be brought about during brief periods when the polar forces are relatively weak, thereby allowing the pushing capability of the spindle to predominate and manifest itself. Alternatively, the spindle could be bent by a momentary reversal in direction of the forces acting on the SPBs.

Could the spindle provide a necessary function by limiting the rate of separation of the SPBs? One possible answer to this question can be derived from a consideration of poleward chromosome migration in Ascomycetes. Chromosomes begin their anaphase migration asynchronously from different points of attachment along the middle two-thirds of the spindle (17, 47). Many chromosomes have reached the pole while others (lagging chromosomes) typically are still near the center of the spindle. A central spindle that restricts the rate of SPB separation to a speed slower than that of poleward migration of the chromosomes would help ensure that both poles would receive the full complement of chromosomes before the nuclear envelope closes behind them.

Our overall concept of force deployment related to the

mitotic cycle in *Fusarium* spp. would have SPB-associated microtubules playing a key role at every step, as was suggested by Poon and Day (31) for a Basidiomycete, *Ustilago violaceae*. At interphase, nuclear migration and position would depend primarily on extranuclear forces exerted on the SPB via astral microtubules (18, 26). During prophase, there are relatively few astral microtubules and the nucleus is relatively quiescent (18). Rotational movements of metaphase nuclei could result from transitory or weak associations of cytoplasmic microtubules with the SPBs (18) or the nuclear envelope (31). Fig. 23 presents diagrammatically our concepts of the forces acting on the SPBs during anaphase and telophase. During anaphase, the kinetochore microtubules would depolymerize at the kinetochores and pull the kinetochores and chromosomes to the poles (17, 18) in a manner analogous to phase I in higher plant and animal mitosis (1, 2, 44). The central spindle, by virtue of the rigidity and growth of its component microtubules, would provide a counterforce against chromosome separation. The force being exerted on the SPBs by astral microtubules would be resisted by intermolecular forces between tubulin subunits in the spindle microtubules. The balance of forces would be tipped slightly in favor of the asters, and some separation of the poles would occur during anaphase, as observed. During early telophase, astral forces would continue to operate, and the rate of separation of the SPBs would be governed primarily by the magnitude of the astral forces and the growth rate of spindle microtubules. During brief periods when the astral forces would wane, the continuing growth of the central spindle microtubules would generate a force that would push the poles farther apart, possibly at a reduced rate. Severing the central spindle by laser microbeam at early telophase would neutralize all of its ascribed forces and counterforces that act on the SPB, tip the balance heavily in favor of astral forces, and result in the observed acceleration in the rate of separation of the SPBs. The increased motility of daughter nuclei that occurs when the spindle breaks, either naturally (17) or as a result of laser irradiation, would simply reflect a continuation of the astral forces that were acting on the SPBs during the previous stages. Once the daughter nuclei had reached an appropriate position in the cell, they would revert to the relatively quiescent interphase condition (17) with a reduced complement of astral microtubules (18; Aist and Berns, unpublished observations). These astral microtubules would facilitate the persistent oscillatory and translational motions that characterize the SPB at interphase (10, 17, 25, 26).

The extent to which our proposed model (Fig. 23) of the mechanics of mitosis in *F. solani* may apply also to other organisms is a matter for future experimentation. It would certainly seem to be a possibility for the numerous other situations where both astral microtubules and a distinct anaphase-telophase elongation of the central spindle occur. Included in this group are numerous fungi (10, 16, 17, 48–57), several slime molds (58–60), some algae (61, 62), certain protozoans (45, 63), and higher animals (1, 2, 9, 11). Girbardt's concept (10) of mitosis in the Basidiomycete, *Trametes versicolor*, is especially concordant. Bergan (9) proposed that the elongating central spindle in fish embryos plays a passive role, while centriole migration—which can occur in the absence of a central spindle—provides the motile force to separate incipient daughter nuclei. In these and other mitoses in which separation of nuclei can occur in the absence of a central spindle (28, 64), polar forces seem almost certain to play a role. Bajer et al. (28) observed that, in certain aberrant mitoses in

cultured lung epithelium from the newt, separation of the spindle poles occurred without interzonal microtubules. They concluded that half-spindles moved autonomously and independently. Moreover, the central spindle during phase II in many organisms besides *Fusarium* spp. is composed of very few, possibly weak, or decreasing numbers, of microtubules (1, 8, 49, 57, 65, 66, 67), which suggests that the motile forces separating the poles in these organisms may not reside principally in the central spindle. Most students of mitosis have assumed that astral forces are inoperative or insignificant with respect to the mechanics of chromosome separation, since a possible role of asters is rarely mentioned. Our results, and those of Bajer et al. (28) and Bergan (9), suggest that this question should now be re-examined on a broad scale.

The bipartite spindle postulated to occur in *F. solani* on the basis of phasecontrast observations of mitosis in living cells (21) is confirmed here by electron microscopy. Olive (53) reported a similar spindle architecture for late anaphase and early telophase in fixed and stained preparations of meiosis I in the rust fungus, *Coleosporium vernoniae*. According to Olive, the chromosomes passed to the spindle poles along these two spindle strands, resulting in a bilobed appearance of the incipient daughter nuclei. We also observed that in living cells the chromosomes migrate along these spindle strands, but it was unclear whether or not all chromosomes were closely associated with a visible strand. The chromosomes in Ascomycetes and Basidiomycetes commonly appear to migrate along two rows at anaphase (17, 18, 68) and incipient daughter nuclei are typically bilobed (69). Since reports of bipartite spindles in fungi are rare, any general relationship between the duality of the spindle and anaphase rows of chromosomes is obscure. Lateral associations of spindle microtubules to form several microtubule bundles is a common occurrence in larger spindles (1, 8), and such associations could be important in the generation of forces that control chromosome separation.

Rotation of the broken halves of the spindle, usually in opposite directions, was a characteristic result of spindle irradiation. This observation is reminiscent of reports that daughter nuclei rotate after natural breakdown of the spindle (70–72) and may indicate that torques of opposite direction are acting on the nuclei during and after phase II. The observed associations of astral microtubules from the two spindle poles with the plasma membrane on opposite sides of the cell presents a possible explanation of these observations; a pulling force transmitted to the SPBs via these microtubules would tend to slant the SPBs toward the lateral walls and rotate the broken spindles or daughter nuclei in opposite directions. The consistent orientation of the SPBs toward the side walls at early telophase, as observed in this study, is interpreted as evidence of this torque. Rotation of individual spindle strands that were selectively severed by the laser is particularly interesting, since it indicates that, under certain conditions, torque can be expressed on only part of the SPB; the SPB can apparently pivot or fold as a result of the pull of astral forces.

We are grateful to L. Liaw and M. Koonce for technical assistance.

Support for this study was provided in part by National Institutes of Health (NIH) grant GM23445-04 and Hatch Project No. 153432. The work was conducted in the NIH Biotechnology Resource Facility supported by NIH grant RRO 11921.

Received for publication 6 April 1981, and in revised form 19 June 1981.

REFERENCES

1. Bajer, A. S., and J. Molé-Bajer. 1972. Spindle Dynamics and Chromosome Movements. *Int. Rev. Cytol. (Suppl. 3)*. Academic Press, Inc., New York.
2. Mazia, D. 1961. Mitosis and the physiology of cell division. In *The Cell*. J. Brachet and A. E. Mirsky, editors. Academic Press, Inc., New York. 3:77-412.
3. Heath, I. B. 1974. Genome separation mechanisms in prokaryotes, algae, and fungi. In *The Cell Nucleus*. H. Busch, editor. Academic Press, Inc., New York. II:487-515.
4. Heath, I. B. 1980. Variant mitosis in lower eukaryotes: indicators of the evolution of mitosis. *Int. Rev. Cytol.* 64:1-80.
5. Kubai, D. F. 1975. The evolution of the mitotic spindle. *Int. Rev. Cytol.* 43:167-277.
6. Bělár, K. 1929. Beiträge zur Kausalanalyse der Mitose. II. Untersuchungen an den Spermatozyten von *Chorthippus (Stenobothrus) lineatus* Panz. *Wilhelm Roux Arch. Entwicklungsmech. Org.* 118:359-484.
7. Bělár, K. 1929. Beiträge zur Kausalanalyse der Mitose. III. Untersuchungen an den Staubfadenhaarzellen und Blatmeristemzellen von *Tradescantia virginica*. *Z. Zellforsch. Mikrosk. Anat.* 10:73-134.
8. Fuge, H. 1977. Ultrastructure of the Mitotic Spindle. *Int. Rev. Cytol. (Suppl. 6)*. Academic Press, Inc., New York. 1-58.
9. Bergan, P. 1960. On the blocking of mitosis by heat shock applied at different mitotic stages in the cleavage division of *Trichogaster trichopterus* var. *sumatranus* (Teleostei: Anabantidae). *Nytt Mag. Zool. (Oslo)*. 9:37-121.
10. Girbard, M. 1968. Ultrastructure and dynamics of the moving nucleus. In *Aspects of Cell Motility*. Twenty-second Symposium of the Society for Experimental Biology, Oxford. Cambridge University Press. 249-259.
11. Sakai, H., Y. Hiramoto, and R. Kuriyama. 1975. The glycerol-isolated mitotic apparatus: a response to porcine brain tubulin and induction of chromosome motion. *Dev. Growth Differ.* 17:265-274.
12. Forer, A. 1978. Chromosome movements during cell-division: possible involvement of actin filaments. In *Nuclear Division in the Fungi*. I. B. Heath, editor. Academic Press, Inc., New York.
13. Fuller, M. S. 1976. Mitosis in fungi. *Int. Rev. Cytol.* 45:113-153.
14. Luyckx, P. 1970. Cellular Mechanisms of Chromosome Distribution. *Int. Rev. Cytol. (Suppl. 2)*. Academic Press, Inc., New York.
15. Heath, I. B. 1980. Fungal mitoses, the significance of variations on a theme. *Mycologia*. 72:229-250.
16. Heath, I. B., and M. C. Heath. 1976. Ultrastructure of mitosis in the cowpea rust fungus *Uromyces phaseoli* var. *vignae*. *J. Cell Biol.* 70:592-607.
17. Aist, J. R. 1969. The mitotic apparatus in fungi, *Ceratocystis fagacearum* and *Fusarium oxysporum*. *J. Cell Biol.* 40:120-135.
18. Aist, J. R., and P. H. Williams. 1972. Ultrastructure and time course of mitosis in the fungus *Fusarium oxysporum*. *J. Cell Biol.* 55:368-389.
19. Aist, J. R., and M. W. Berns. 1980. Function of the post-anaphase spindle of fungi: a laser microbeam study. *J. Cell Biol.* 87(2, Pt. 2):234a (Abstr.).
20. Strahs, K. R., J. M. Burt, and M. W. Berns. 1978. Contractility changes in cultured cardiac cells following laser microirradiation of myofibrils and the cell surface. *Exp. Cell Res.* 113: 75-83.
21. Aist, J. R. 1974. Nuclear division in fungi. *Proceedings of the First Intersectoral Congress of International Association of Microbiological Societies*. 2:102-106.
22. Howard, R. J., and J. R. Aist. 1979. Hyphal tip cell ultrastructure of the fungus *Fusarium*: improved preservation by freeze-substitution. *J. Ultrastruct. Res.* 66:224-234.
23. Berns, M. W., N. Gamajala, R. Olson, C. Duffy, and D. E. Rounds. 1970. Argon laser micro-irradiation of mitochondria in rat myocardial cells in tissue culture. *J. Cell. Physiol.* 76:207-214.
24. Aist, J. R. 1976. Papillae and related wound plugs of plant cells. *Annu. Rev. Phytopathol.* 14:145-163.
25. Thielke, Ch. 1975. *Fusarium solani* (Fungi imperfecti) Intranucleäre Mitose. Encyclopaedia Cinematographica E 2179/1975. G. Wolf, editor. Institut für den wissenschaftlichen Film, Göttingen. 1-8.
26. Wilson, C. L., and J. R. Aist. 1967. Motility of fungal nuclei. *Phytopathology*. 57:769-771.
27. Bakerspigel, A. 1973. Nuclei in the somatic hyphae of *Trichophyton mentagrophytes*. *Can. J. Microbiol.* 19:223-229.
28. Bajer, A. S., M. DeBrabander, J. Molé-Bajer, S. Paulaitis, and H. Howard. 1980. Monopolar division, aster motility and anaphase-like movements of prometaphase chromosomes. *J. Cell Biol.* 87(2, Pt. 2):237a (Abstr.).
29. Heath, I. B. 1981. Nucleus-associated organelles in fungi. *Int. Rev. Cytol.* 69:191-221.
30. Nakai, Y., and R. Ushiyama. 1978. Fine structure of shiitake, *Lentinus edodes*. VI. Cytoplasmic microtubules in relation to nuclear movement. *Can. J. Bot.* 56:1206-1211.
31. Poon, N. H., and A. W. Day. 1976. Somatic nuclear division in the sporidia of *Ustilago violacea*. IV. Microtubules and the spindle-pole body. *Can. J. Microbiol.* 22:507-522.
32. Allen, E. D., and A. S. Sussman. 1978. Presence of an actin-like protein in mycelium of *Neurospora crassa*. *J. Bacteriol.* 135:713-716.
33. Heath, I. B., and M. C. Heath. 1978. Microtubules and organelle movements in the rust fungus *Uromyces phaseoli* var. *vignae*. *Cytobiologie*. 16:393-411.
34. Crackower, S. H. B. 1972. The effects of griseofulvin on mitosis in *Aspergillus nidulans*. *Can. J. Microbiol.* 18:683-687.
35. Künkel, W. 1979. Antimitotische Aktivität von Methylbenzimidazol-2-ylcarbamate (MBC). II. Elektronenmikroskopische Untersuchungen zur Duplikation des Kern-assoziierten Organells ("centriolar plaque", "MTOC", "CKE") bei *Aspergillus nidulans*. *Protoplasma*. 101:317-329.
36. Griffith, L. M., and T. D. Pollard. 1978. Evidence for actin filament-microtubule interaction mediated by microtubule-associated proteins. *J. Cell Biol.* 78:958-965.
37. Wang, E., R. K. Cross, and P. W. Choppin. 1979. Involvement of microtubules and 10-nm filaments in the movement and positioning of nuclei in syncytia. *J. Cell Biol.* 83:320-337.
38. Howard, R. J. 1981. Ultrastructural analysis of hyphal tip cell growth in fungi: spitzkörper, cytoskeleton and endomembranes after freeze-substitution. *J. Cell Sci.* 48:89-103.
39. Doohan, M. E., and B. A. Palevitz. 1980. Microtubules and coated vesicles in guard-cell protoplasts of *Allium cepa* L. *Planta (Berl.)*. 149:389-401.
40. Marchant, H. J. 1978. Microtubules associated with the plasma membrane isolated from protoplasts of the green alga *Mougeotia*. *Exp. Cell Res.* 115:25-30.
41. Moore, P. B., C. L. Ownby, and K. L. Carraway. 1978. Interactions of cytoskeletal elements with the plasma membrane of Sarcoma 180 ascites tumor cells. *Exp. Cell Res.* 115:331-342.
42. Griffin, J. L., M. N. Stein, and R. E. Stowell. 1969. Laser microscope irradiation of *Physarum polycephalum*: dynamic and ultrastructural effects. *J. Cell Biol.* 40:108-119.
43. Hatano, S., K. Owaribe, F. Matsumura, and T. Hasegawa. 1980. Characterization of actin, actinin, and myosin isolated from *Physarum*. *Can. J. Bot.* 58:750-759.
44. McIntosh, J. R., P. K. Hepler, and D. G. Van Wie. 1969. Model for mitosis. *Nature (London)*. 224:659-663.
45. Cleveland, L. R. 1966. Reproduction by binary and multiple fission in *Gigantomonas*. *J. Protozool.* 13:573-585.
46. Von Stosch, H. A., and G. Drebes. 1965. Der Stemmkörper und andere Besonderheiten der Diatomeenzytologie. *Naturwissenschaften*. 52:311-312.
47. Robinow, C. F., and C. E. Caten. 1969. Mitosis in *Aspergillus nidulans*. *J. Cell Sci.* 5:403-431.
48. Harper, R. A. 1905. Sexual Reproduction and the Organization of the Nucleus in Certain Mildews. Carnegie Institution of Washington, Publication no. 37.
49. Heath, I. B., and A. D. Greenwood. 1970. Centriole replication and nuclear division in *Saprolegnia*. *J. Gen. Microbiol.* 62:139-148.
50. Huang, H. C., R. O. Tinline, and L. C. Fowke. 1975. Ultrastructure of somatic mitosis in a diploid strain of the plant pathogenic fungus *Cochliobolus sativus*. *Can. J. Bot.* 53:403-414.
51. Ichida, A. A., and M. S. Fuller. 1968. Ultrastructure of mitosis in the aquatic fungus *Catenaria anquillulae*. *Mycologia*. 60:141-155.
52. McNit, R. 1973. Mitosis in *Phycoctytrium irregulare*. *Can. J. Bot.* 51:2065-2074.
53. Olive, L. S. 1949. Karyogamy and meiosis in the rust *Coleosporium vernoniae*. *Am. J. Bot.* 36:41-54.
54. Poon, N. H., and A. W. Day. 1976. Somatic nuclear division in the sporidia of *Ustilago violacea*. III. Ultrastructural observations. *Can. J. Microbiol.* 22:495-506.
55. Powell, M. J. 1980. Mitosis in the aquatic fungus *Rhizophyidum spherotheca* (Chytridiales). *Am. J. Bot.* 67:839-853.
56. Robinow, C. F., and J. Marak. 1966. A fiber apparatus in the nucleus of the yeast cell. *J. Cell Biol.* 29:129-151.
57. Whisler, H. C., and L. B. Travland. 1973. Mitosis in *Harpochytrium*. *Arch. Protistenkd.* 115:69-74.
58. Hinchee, A. A., and E. F. Haskins. 1980. Open spindle nuclear division in the amoebal phase of the acellular slime mold *Echinostelium minutum* with chromosomal movement related to the pronounced rearrangement of spindle microtubules. *Protoplasma*. 102:117-130.
59. Moens, P. B. 1976. Spindle and kinetochore morphology of *Dictyostelium discoideum*. *J. Cell Biol.* 68:113-122.
60. Roos, U.-P. 1975. Mitosis in the cellular slime mold *Polysphondylium violaceum*. *J. Cell Biol.* 64:480-491.
61. McDonald, K. 1972. The ultrastructure of mitosis in the marine red alga *Membranoptera platyphylla*. *J. Phycol.* 8:156-166.
62. Pickett-Heaps, J. D., K. L. McDonald, and D. H. Tippit. 1975. Cell division in the pennate diatom *Diatoma vulgare*. *Protoplasma*. 86:205-242.
63. Cleveland, L. R. 1953. Studies on chromosomes and nuclear division. *Trans. Am. Philos. Soc.* 43:809-869.
64. Dubremetz, J. F. 1973. Etude ultrastructurale de la mitose schizogonique chez la coccidie *Eimeria necatrix* (Johnson 1930). *J. Ultrastruct. Res.* 42:354-376.
65. Fuge, H. 1974. Ultrastructure and function of the spindle apparatus microtubules and chromosomes during nuclear division. *Protoplasma*. 82:289-320.
66. Sakai, A., and M. Shigenaga. 1972. Electron microscopy of dividing cells. IV. Behavior of spindle microtubules during nuclear division in the plasmodium of the myxomycete *Physarum polycephalum*. *Chromosoma (Berl.)*. 37:101-116.
67. McIntosh, J. R., K. L. McDonald, M. K. Edwards, and B. M. Ross. 1979. Three-dimensional structure of the central mitotic spindle of *Diatoma vulgare*. *J. Cell Biol.* 83: 428-442.
68. Setliff, E. C., H. C. Hoch, and R. F. Patton. 1974. Studies on nuclear division in basidia of *Poria latemarginata*. *Can. J. Bot.* 52:2323-2333.
69. Goates, B. J., and J. A. Hoffmann. 1979. Somatic nuclear division in *Tilletia* species pathogenic on wheat. *Phytopathology*. 69:592-598.
70. Bakerspigel, A. 1958. The structure and mode of division of the nuclei in the vegetative spores, and hyphae of *Endogone spagnophila* Atk. *Am. J. Bot.* 45:404-410.
71. Bakerspigel, A. 1969. Cytological problems in *Candida albicans*. In *Yeasts. Proceedings of the Second Symposium on Yeasts* (1966). Bratislava, Czechoslovakia. 187-192.
72. McCully, E. K., and C. F. Robinow. 1971. Mitosis in the fission yeast *Schizosaccharomyces pombe*: a comparative study with light and electron microscopy. *J. Cell Sci.* 9:475-507.